Int. J. Electrochem. Sci., 6 **(2011)** 2022 - 2030

International Journal of
ELECTROCHEMICAL
SCIENCE
www.electrochemsci.org

Synthesis of Nano-$LiMnPO_4$ from $MnPO_4 \cdot H_2O$ Prepared by Mechanochemistry

Li Wang, Wenting Sun, Xiangming He[*], Jianjun Li, Changyin Jiang

Beijing Key Lab of Fine Ceramics, Institute of Nuclear and New Energy Technology, Tsinghua University, Beijing 100084, PR China
[*]E-mail: hexm@tsinghua.edu.cn;

Received: 8 April 2011 / *Accepted:* 15 May 2011 / *Published:* 1 June 2011

Synthesis of nano-$LiMnPO_4$ from $MnPO_4 \cdot H_2O$ prepared by mechanochemistry is attempted. SEM, TEM, XRD and TG/DSC are performed to characterize the products. The results show that the primary particles are loosely aggregated with an average particle size of 40-50 nm. The morphology and particle size distribution of nano-$LiMnPO_4$ preserves those of $MnPO_4 \cdot H_2O$. This paves a promising way of high efficiency, easy accessibility and speediness to prepare nano-$LiMnPO_4$.

Keywords: $MnPO_4$, nano-cystalline, mechanochemistery, $LiMnPO_4$, lithium-ion batteries

1. INTRODUCTION

The synthesis of inorganic nanocrystals has attracted considerable interest due to dramatic improvements caused by nano-effect [1,2]. Olivine $LiMnPO_4$ is now recognized as a promising cathode material for lithium ion batteries with potential vehicular application because of low cost, environmentally benign constituents and high theoretical capacity. Compared with the popular $LiFePO_4$ cathode material [3-9], $LiMnPO_4$ is of particular interest to the battery community because of the ideal location of the Mn^{2+}/Mn^{3+} couple at 4.1 V vs. Li/Li^+, which is 0.65V higher than $LiFePO_4$, and its theoretical energy density (684Wh/kg = 171mAh/g × 4.0V) is 1.2 times larger than that of $LiFePO_4$ (578Wh/kg = 170mAh/g × 3.4V).

The main drawback of $LiMnPO_4$ is their low electronic conductivity, which results in poor rate capability. Since Li et al.[10] first reported the reversible reaction of Mn(II)↔Mn(III) in olivine phosphate, researchers have tried various methods to prepare electro-active $LiMnPO_4$ to overcome the limitation on its application. Encouraged by the successful studies on $LiFePO_4$, developing specific synthesis methods appropriating for designing LiMnPO4 in the nano-scale region is in great need to improve the kinetics of $LiMnPO_4$, as it has been proved that decreasing the size of the crystallites to nano-scale offers potential for higher electrode/electrolyte surface contact, less mechanical strain upon lithium (de)intercalation from the lattice than the bulk materials and reduces path length for lithium-ion/electron transport through the material [11, 12]. Nano-$LiMnPO_4$ is generally realized by three synthetic routes. Sol-gel method is a typical one, by which nano-$LiMnPO_4$ was realized using precursor with atomic or molecular uniformity [13, 14]. Drezen et al. [15] explored sol-gel method to prepare nano-$LiMnPO_4$. Their results showed that $LiMnPO_4$ with 200nm and 270nm average particles size presented 79 mAh g^{-1} at $C/5$, while $LiMnPO_4$ with 140nm average particles size presented the reversible capacity up to 116 mAh g^{-1} at $C/5$. Another synthetic route is direct precipitation of $LiMnPO_4$ in liquid-phase [16-20], among which solvothermal and refluxing using high-boiling-point organic solution are more popular. These methods allow preparing $LiMnPO_4$ with tiny but uniform particle size and controllable morphology. Wang et al. and Grazel [19, 21] presented platelet-like $LiMnPO_4$ with the high specific capacity of 159 mAh g^{-1} at C/10 and 138 mAh g^{-1} at 1C. The excellent electrochemical performance was ascribed to the platelet morphology, which gave a very short distance of less than 30nm for Li^+ diffusion. Solvothermal method was attracted to synthesis $LiMnPO_4/C$ nanocomposite with a uniform particle dimension which delivered an initial discharge capacity of 126.5 mAh g^{-1} [22].

Solid-state reaction using nano-scale precursor is the most widely used synthetic route for industry, due to its advantages such as easy operation, easy adjustment of composition and being appropriate for scale production. Especially, solid-state reaction is generally necessary since it helpful to form effective surface layer on the materials. Rapid and effective method for preparing nano-precursor is essential. In this study, a mechanochemical method was introduce to prepare uniform nano-$MnPO_4 \cdot H_2O$. On that basis, nano-$LiMnPO_4$ was prepared and evaluated.

2. EXPERIMENTAL

0.08mol 50% $Mn(NO_3)_2$ was dissolved in 80ml anhydrous ethanol. Then 20ml 70% H_3PO_4 was added into the solution and stirred. A suitable amount of urea was used to adjust the PH value. These materials were mixed at room temperature. The following ball milling procedure was carried out in a planetary-type ball mill (500 rpm). After 0.5-1 hour, the products were washed and dried. Nano-$LiMnPO_4$ was prepared by solid-state carbon thermal reduction. A stoichiometric amount of $MnPO_4 \cdot H_2O$, $LiCOOCH_3 \cdot 2H_2O$ and 10% excess sucrose were mixed in the agate mortar. Then the mixture was calcined at 500°C for 4 h in flowing ultra-pure Ar or N_2 to obtain nano-$LiMnPO_4$ material.

The products were characterized by X-ray diffraction pattern (XRD, D/max 2550V, Rigaku, Japan) with Cu-Kα irradiation (λ=1.5406 nm). The morphology of the samples was inspected using scanning electron microscope (SEM, JSM-5600LV, JEOL, Japan) and transmission electron microscope (TEM, H-800, Hitachi, Japan). A combined differential scanning calorimetry/thermogravimetric analysis (DSC/TGA) instrument (Netzsch, STA 449C) was used to study the decomposition and reaction of the precursors. The powder sample of $MnPO_4$ and the mixture of the starting materials for preparing $LiMnPO_4$ were heated in an argon reducing environment to

900°C at a ramp rate of 5°C/min. The electrochemical characterization was performed using CR2032 coin-type test cells. The test electrode was prepared from a mixture consisting of 80wt% $LiMnPO_4/C$, 10wt% acetylene black, and 10 wt% PVDF. After rolling using rolling machine for several times, the mixture was cut into slices as test electrode. A Li-foil and a polypropylene film (Celgard 2400) were used as the counter electrode and separator, respectively. The electrolyte was 1mol L^{-1} $LiPF_6$/EC+DMC+DEC (3:3:1 by volume). The prepared electrode pellets were dried at 120 °C under vacuum for 48 h. ell assembly was conducted under an Ar atmosphere with a dew point below -70 °C. The charge/discharge model was chosen constant current mode (CC mode). In this mode, the cells were charge–discharge cycled over a cell-voltage window of between 3V and 4.5V at a constant current (2.5 mA g^{-1}) at room temperature.

3. RESULTS AND DISCUSSION

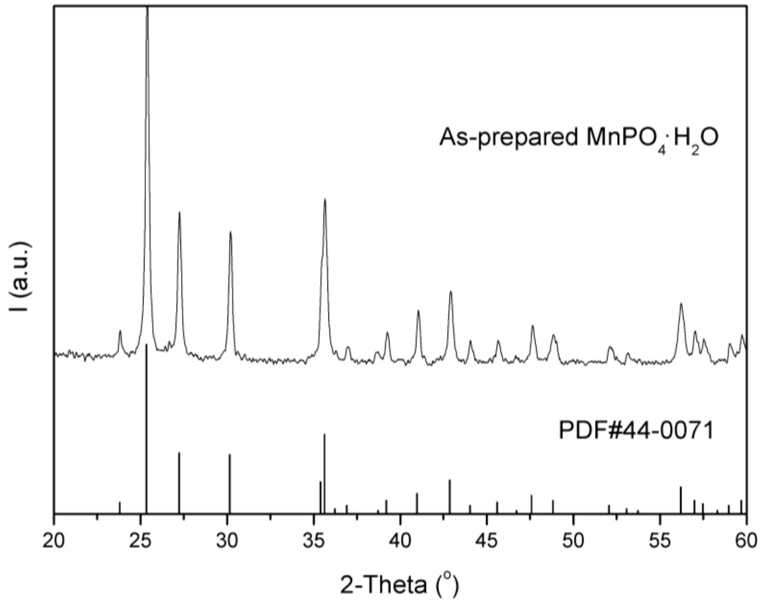

Figure 1. XRD pattern of as-prepared $MnPO_4 \cdot H_2O$

Figure 1 shows the XRD pattern of as-prepared $MnPO_4 \cdot H_2O$. All the diffraction peaks in the pattern are in agreement with those of $MnPO_4 \cdot H_2O$ (PDF card 00-044-0071). The relative intensity of diffraction peaks of is similar to the standard patterns, indicating that no preferentially growing directions for samples prepared by mechanochemical method. No characteristic peaks of impurity phases are present, indicating the high purity of the samples. It profited from the suitable pH condition. During the soft mechanochemical process, reactions take place as follows:

$$Mn^{2+} + 4H^{+} + NO_3^{-} + PO_4^{3-} \rightarrow MnPO4 \cdot H_2O\downarrow + NO\uparrow + H_2O \qquad (1)$$

Generally, $MnPO_4·H_2O$ can be easily precipitated at room temperature, as long as high acidity can be satisfied since oxidization of Mn^{2+} to Mn^{3+} by NO_3^- can happen only in high acidity conditions. But high acidity also results in uncontrollable reaction rate, so causes too large particle size, random morphology and wide size distribution. So successful preparation of nano-$MnPO_4·H_2O$ crystalline with good uniformity was seldom reported. For example, Zhang et al. [23] prepared rod-like $MnPO_4·H_2O$ single crystals by hydrothermal method. Though the average diameter is about 68 nm, the rods are closely packed. Boonchom et al. [24] used a simple precipitation route at low temperature to synthesis nanocrystalline $MnPO_4·H_2O$. Various attempts as they tried, the as prepared $MnPO_4·H_2O$ was nonuniform polyhedral grains and badly aggregated.

To obtain uniform nano-$MnPO_4·H_2O$ particles, two design are introduced in our work. The first one is using ethanol as inert solvents to reduce both producing rate and growing rate. The second one is using a soft ball-milling to introduce local heating and large amounts of nucleate surface, so that to confine the formation of $MnPO_4·H_2O$ only on the collision surfaces. By tuning aqueous content and milling speed, particle size of nano-$MnPO_4·H_2O$ can be well controlled.

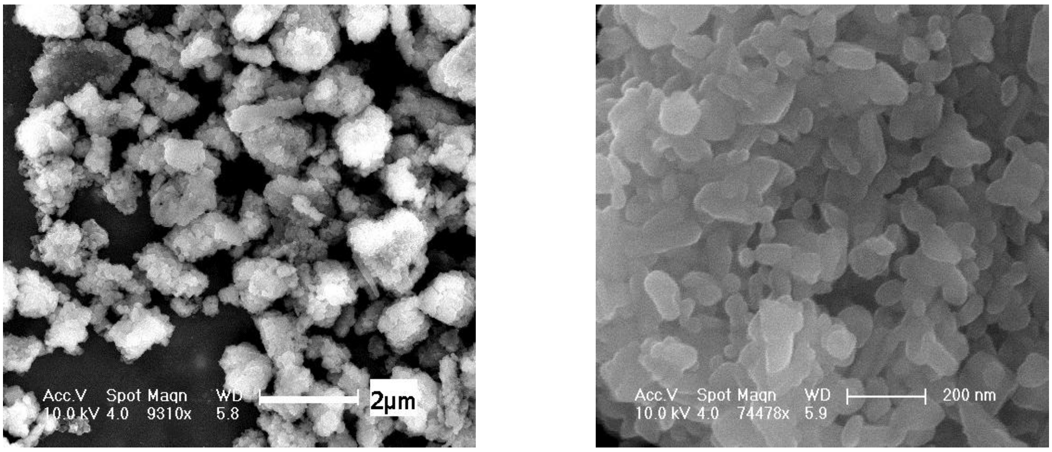

Figure 2. SEM photographs of as-prepared $MnPO_4·H_2O$

From SEM photographs of the nano-$MnPO_4·H_2O$, it can be observed that the sample consists of secondary particles which are random in shape. These secondary particles are formed by loose aggregation of primary particles. The TEM image shows that the primary particle size ranges from 40 to 50 nm. It is worth to be noted that the products present both uniform nano-size and pure $MnPO_4·H_2O$ crystalline phase.

$MnPO_4·H_2O$ is a good candidate for Mn-contained precursor for $LiMnPO_4$ preparation, since the locations of structural bounded water in $MnPO_4·H_2O$ is close to those of Li atoms in $LiMnPO_4$. This similarity allows a transformation from $MnPO_4·H_2O$ into $LiMnPO_4$ without major structural rearrangements. That is, the size distribution and morphology of $LiMnPO_4$ can be easily controlled by designing those of $MnPO_4·H_2O$. Xiao et al. [25] synthesized $LiMnPO_4/C$ composites with good performance using $MnPO_4·H_2O$ as the precursor which prepared by a precipitation process. As reported, $MnPO_4{\cdot}H_2O$ will thermally decomposed into $Mn_2P_2O_7$, the thermal behaviors of nano-$MnPO_4{\cdot}H_2O$ is essential for preparing nano-$LiMnPO_4$ from nano-$MnPO_4{\cdot}H_2O$.

Figure 3 shows the TG/DSC results of as-prepared nano-$MnPO_4{\cdot}H_2O$ and the precursor mixtures for $LiMnPO_4$. It is worthy for confirming the annealing program for $LiMnPO_4$ preparation, as well as getting information about water content in nano-$MnPO_4{\cdot}H_2O$ precursor which influences the final stoichiometry of the final $LiMnPO_4$ product [26]. According to The TG curve in Fig. 3A, there is only one weight loss of 15.45% by mass lies between 380 and 500°C. Besides, the weight loss is accompanied by a change of color from dark greenish black to pale yellowish white. The DSC curve in Fig. 3A also shows one step exothermic process, which lies in the similar temperature range to that of weight loss. Above results both coincide with the description in literatures [24, 26, 27], indicating that thermal decomposition reaction as happened as follows:

$$4MnPO_4{\cdot}H_2O \rightarrow 2Mn_2P_2O_7 + O_2 + 4H_2O \qquad (2)$$

Especially, the theoretical weight loss is 15.48% according to the reaction, including 4.76% from O_2 and 10.72 from H_2O. The weight loss calculated based on Fig. 3A is 15.45%, indicating that all the water in the as-prepared $MnPO_4{\cdot}H_2O$ are existed as bounded water. Moreover, both TG and DSC curves show peak position around 473.3°C, which is nearly 40°C lower than bulk $MnPO_4{\cdot}H_2O$. This can be attributed to nano-effects, and from which it can be deduced that the annealing temperature can be reduced for nano-$MnPO_4{\cdot}H_2O$ materials when compared with bulk $MnPO_4{\cdot}H_2O$ materials.

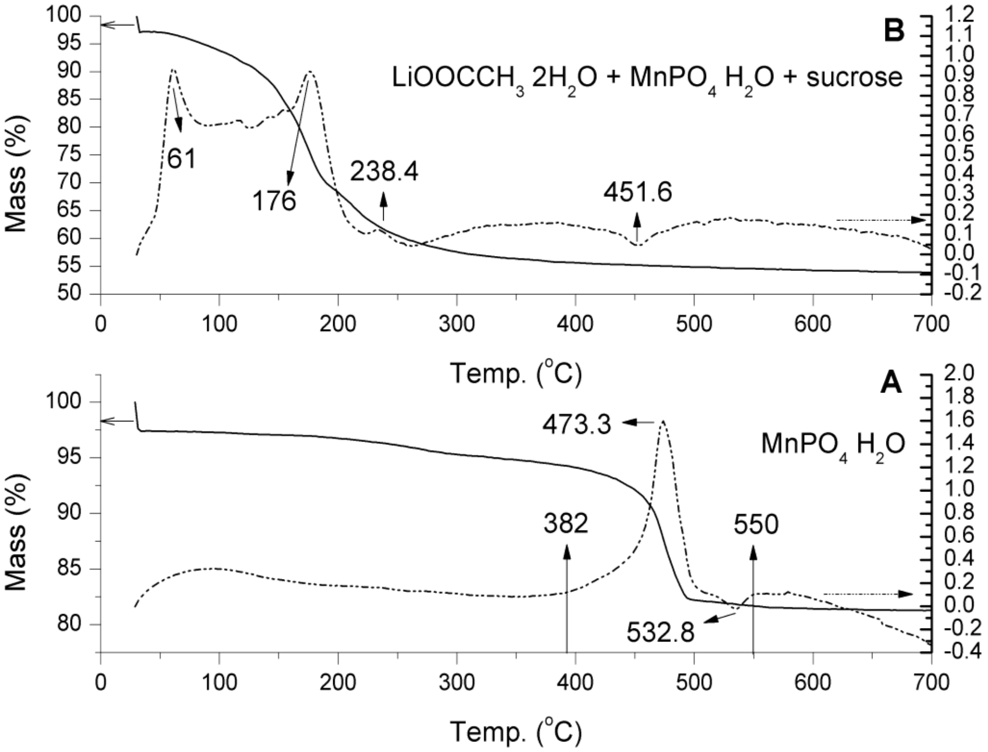

Figure 3. TG/DSC curves of $MnPO_4{\cdot}H_2O$ powders measured in argon

Fig. 3B shows the TG/DSC curves of precursor mixtures. Compared with Fig. 3A, the curves changed greatly both in peak shapes and peak positions. According to the TG curve, there is only one step weight loss, which is 43.59% in mass and lies from 70°C to 300°C. Exactly, the theoretical weight loss is 43.36% according to $LiMnPO_4$ formation reaction. Though the DSC curve is too complex to be understood at temperatures lower than 300°C, it can be known from Fig. 3B that $LiMnPO_4$ formed below 300°C and annealing temperature about 500°C may be appropriate to promote the crystalline growth of $LiMnPO_4$.

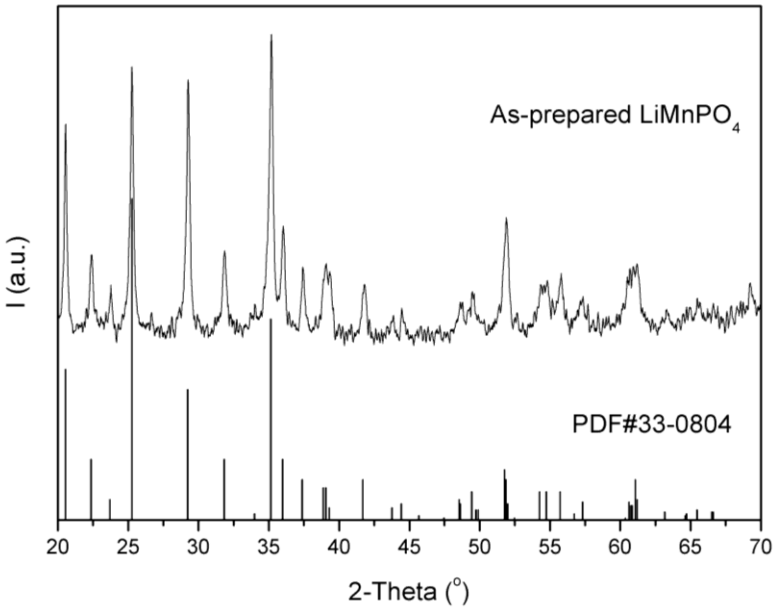

Figure 4. XRD patterns of as-prepared $LiMnPO_4$ powders

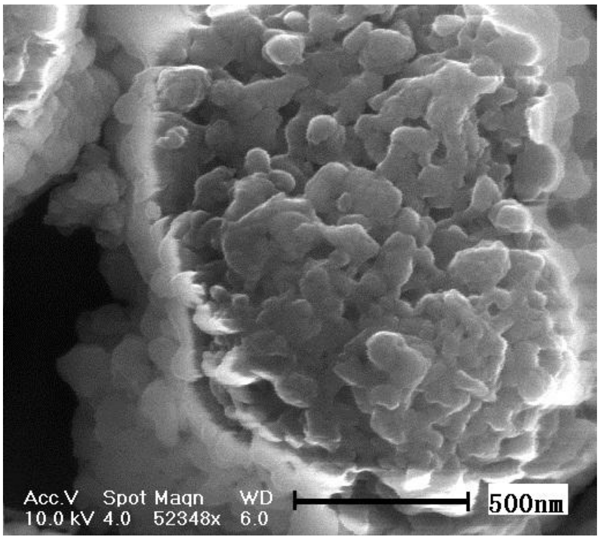

Figure 5. SEM photograph of as-prepared $LiMnPO_4$ powders

The XRD pattern of as-prepared $LiMnPO_4$ was shown in Fig. 4. All the diffraction peaks in the patterns are in agreement with $LiMnPO_4$ (PDF card #33-0803), which is olivine structure indexed in *Pnma* of an orthorhombic system. In the traditional solid state reaction process for preparing $LiMnPO_4$, Li_3PO_4 impurities may easily form during the calcination process. [28] However, the presence of the $MnPO_4 \cdot H_2O$ precursor can significantly reduce the impurities produced by the solid state reaction [25]. Because the polyanion PO_4^{3-} in the $MnPO_4 \cdot H_2O$ has formed a stable structure which PO_4^{3-} tetrahedra and MnO_6 octahedra share the corner oxygen ion, and cannot be react with lithium ion alone.

The SEM photograph of as-prepared nano-$LiMnPO_4$ powders is shown in Fig.5. A little different from expected, It can be found that the morphology of nano-$LiMnPO_4$ was not as consistent as those of nano-$MnPO_4 \cdot H_2O$ precursor. Compared with nano-$MnPO_4 \cdot H_2O$ precursor, the average particle size of primary particles of nano-$LiMnPO_4$ are increased to 40-100 nm. Furthermore, though the secondary particles of nano-$LiMnPO_4$ are also formed by aggregation of the primary particles and random in size, while the dispersity of the primary particles obviously decreased. The difference in morphology and dispersity between nano-$MnPO_4 \cdot H_2O$ powder and nano-$LiMnPO_4$ powder can be attributed to the nonuniformity of solid-state reaction among nano-$MnPO_4 \cdot H_2O$ particles, micro-size sucrose particles and micro-size $LiCOOCH_3 \cdot 2H_2O$ particles. It can be expected that $LiMnPO_4$ powder can keep consistent in morphology and dispersity with nano-$MnPO_4 \cdot H_2O$ when all the reactants are in nanosize and well mixed. Further work in this aspect needs to be explored. Besides, the as-prepared nano-$LiMnPO_4$ particles are neat and no amorphous carbon can be observed, indicating that sucrose is almost exhausted during thermo-reduction. Since bare $LiMnPO_4$ can hardly present good electrochemical performances even in nano-size due to poor electronic conductivity, more sucrose should be used to form $LiMnPO_4$/C composites in our future study.

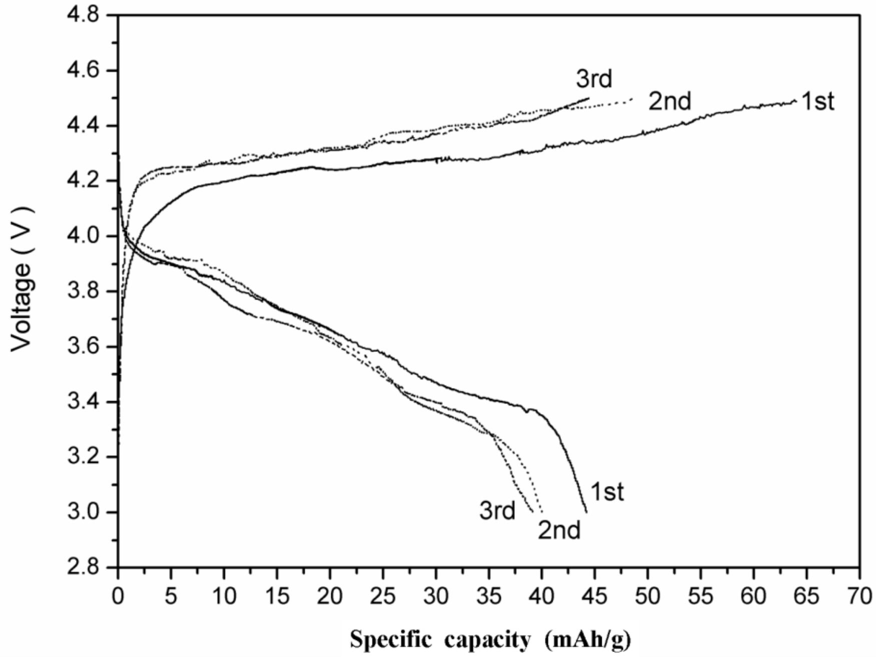

Figure 6. Charge and discharge curves of as-prepared $LiMnPO_4$ powders

Fig.6 showed the charge-discharge curves of as-prepared nano-$LiMnPO_4$, with cycling voltage of 3V- 4.5V and a constant current density of 2.5 mA g^{-1}. As can be seen in Fig.4, rather than small voltage plateau at 4.2 V and 3.9 V for charging and discharging curves respectively, the voltage shows a continuous change for both processes. And this is far different with the theoretical behaviors of Mn^{2+}/Mn^{3+} couple. Besides, the reversible capacity is about 40 mAh g^{-1}. All of the phenomena mean that the as-prepared nano-$LiMnPO_4$ suffers from bad polarizations during the lithiation/delithiation reaction. Keeping in mind that the particle sizes are very small as shown in Fig. 4, it seems more reasonable to attribute low utilization and high polarization of $LiMnPO_4$ to sluggish kinetics of lithium transport within the particles rather than too long diffusion lengths. It is believed that this can be improved by compositing nano- $LiMnPO_4$ particles with conductive carbonous materials. On the other hand, it is reported that for nano-materials, two-phase equilibrium reactions tend to turn into solid solution, presenting a continuous change in voltage should be observed in charge and discharge curves [29, 30]. A large irreversible capacity observed especially during the first cycling is most likely due to the oxidation of the electrolyte at relatively high cut-off voltage. [31] Some reports have demonstrated that the adding of carbon to the reactants and ball-milling before annealing enhances the electrochemical performance. [32] Further research was in progress. Anyway, the above results demonstrated that electrochemically active $LiMnPO_4$ can be obtained by this method.

4. CONCLUSION

Nano-$MnPO_4 \cdot H_2O$ can be successfully prepared by a soft mechanochemical method for the first time. The as-prepared nano-$LiMnPO_4$ consisted of uniform particles with narrow size distribution. Nano-$LiMnPO_4$ is prepared using this nano-$MnPO_4 \cdot H_2O$ as precursor. Though the reversible capacity is only 40 mAh g^{-1}, it is evident that electrochemically active nano-$LiMnPO_4$ can be obtained by this method and applicable electrochemical performance will be reached by optimizing preparation process only.

ACKNOWLEDGEMENT
This work is supported by the NSFC (Grand No.20901046), the State Key Project of Fundamental Research for Nanoscience and Nanotechnology (Grant No. 2011CB935902) and the State Key Project of International Cooperation (Grant No. 2010DFA72760).

References

1. Ganjali M R, Poursaberi T, Khoobi M, Shafiee A, Adibi M, Pirali-Hamedani M, Norouzi P, *Int. J. Electrochem. Sci.* 6 (2011) 717-726.
2. Mai L Q, Gao Y, Guan J G, Hu B, Xu L, Jin W, *Int. J. Electrochem. Sci*. 4 (2009) 755-761.
3. B. Ellis, Wang Hay Kan, W. R. M. Makahnouk, L. F. Nazar, *J. Mater. Chem*. 17 (2007) 3248–3254.
4. Dominko R, Bele M, Gaberscek M, Remskar M, Hanzel D, Pejovnik S, Jamnik J, *J. Electrochem. Soc.* 152 (2005) A607-A610.
5. Huang H, Yin S C, Nazar L F, *Electrochem. Solid-State Lett*. 4 (2001) a170-a172.
6. Chung S Y, Bloking J T, Chiang Y M, *Nat. Mater.*1 (2002) 123-128.

7. A.Vadivel Murugan, T. Muraliganth, A. Manthiram, *J. Phys. Chem. C.* 112 (2008) 14665-14671.
8. Gangulibabu, Kalaiselvi N, Bhuvaneswari D, Doh CH, *Int. J. Electrochem. Sci.* 5 (2010) 1597-1604.
9. Jayaprakash N, Kalaiselvi N, Periasamy P, *Int. J. Electrochem. Sci*. 3 (2008) 476-488.
10. Guohua Li, Hideto Azuma, Masayuki Tohda, *Electrochem. Solid-State Lett*. 5 (2002) A135-A137.
11. Zhumabay Bakenov, Izumi Taniguchi, *Electrochem. Commun*. 12 (2010) 75–78.
12. Daiwon Choi, Donghai Wang, In-Tae Bae, Jie Xiao, Zimin Nie, Wei Wang, Vilayanur V. Viswanathan, Yun Jung Lee, Ji-Guang Zhang, Gordon L. Graff, Zhenguo Yang, Jun Liu, *Nano Lett.* 10 (2010) 2799–2805.
13. V. Koleva, R. Stoyanova, E. Zhecheva, *Mater. Chem. Phys*. 121 (2010) 370–377.
14. Seung-Min Oha, Sung Woo Oha, Seung-Taek Myungb, Sung-Man Leec, Yang-Kook Suna, *J. Alloys Compd.* 506 (2010) 372–376.
15. T. Drezen, N.-H. Kwon, P. Bowen, I. Teerlinck, M. Isono, I. Exnar, *J. Power Sources* 174 (2007) 949–953.
16. C. Delacourt, P. Poizot, M. Morcrette, J.-M. Tarascon, C. Masquelier, *Chem. Mater*. 16 (2004) 93-99.
17. Takayuki Doi, Shota Yatomi, Tetsuya Kida,Shigeto Okada, Jun-ichi Yamaki, *Cryst. Growth Des*. 9 (2009) 4990-4992.
18. T.R. Kim, D.H. Kim, H.W. Ryu, J.H. Moon, J.H. Lee, S. Boo, J. Kim, *J. Phys. Chem. Solids*. 68 (2007) 1203-1206.
19. D. Wang, H. Buqa, M. Crouet, G. Deghenghi, T. Dreen, I. Exnar, N.-H. Kwon, J.H. Miners, L. Poletto, M. Graetzel, *J. Power Sources*, 189 (2009) 624-628.
20. Haisheng Fang, Liping Li, Yong Yang, Guofeng Yan, Guangshe Li, Chem. *Commun*. (2008) 1118-1120.
21. N.-H. Kwon, T. Drezen, I. Exnar, I. Teerlinck, M. Isono, M. Grätzel, *Electrochem. Solid-State Lett*. 9 (2006) A277–A280.
22. Yourong Wang, Yifu Yang, Yanbo Yang, Huixia Shao, *Solid State Commun*. 150 (2010) 81-85.
23. Yuanguang Zhang, Yi Liu, Shengquan Fu, Fan Guo, Yitai Qian, *Bull. Chem. Soc. Jpn*. 79 (2006) 270-275.
24. Banjong Boonchom, Sujittra Youngme, Santi Maensiri, Chanaiporn Danvirutai, *J. Alloys Compd.* 454 (2008) 78-82.
25. Jie Xiao, Wu Xu, Daiwon Choi, Ji-Guang Zhang, *J. Electrochem. Soc.* 157 (2010) A142-A147.
26. Banjong Boonchom, Rattanai Baitahe, Zongporn Joungmunkong, Naratip Vittayakorn, *Powder Tech*. 203 (2010) 310–314.
27. Thomas Witzke, Reinhard Wegner, Thomas Doering, Herbert Pollmann, *Walter Schuckmann, American Mineralogist*, 85 (2000) 847-849.
28. H. Fang, Z. Pan, L. Li, Y. Yang, G. Yan, G. Li, S. Wei, *Electrochem. Commun*. 10 (2008) 1071-1073.
29. P. Ramesh Kumar, M. Venkateswarlu,b Manjusri Misra, Amar K. Mohanty, N. Satyanarayanaa, *J. Electrochem. Soc*. 158 (2011) A227-A230.
30. Guoying Chen, Thomas J. Richardson, *J. Electrochem. Soc.* 156 (2009) A756-A762.
31. Haisheng Fang, Liping Li, Guangshe Li, *Chem. Lett*. 36 (2007) 436-437.
32. N. N. Bramnik, H. Ehrenberg, *J. Alloys Compd*. 464 (2008) 259-264.